10th World Congress on Structural and Multidisciplinary Optimization
May 19 -24, 2013, Orlando, Florida, USA

Optimal Cross Sections for Cold Formed Steel Members under Compression

Mohammadreza M. Gargari[1], Arghavan Louhghalam[2], M. Tootkaboni[1]

[1] University of Massachusetts Dartmouth, North Dartmouth, MA, USA, mmoharramigargari@umassd.edu
[2] Massachusetts Institute of Technology, Cambridge, MA, USA, arghavan@mit.edu

Abstract
Cold formed steel (CFS) has many advantages over other construction materials. CFS members are lightweight. They weigh up to 35-50% less than their wood counterparts. High strength and stiffness to weight ratio is another advantage. This makes CFS members economical and the same time very easy to erect and install (almost no framework is needed). CFS is very durable, is not combustible, is easy to transport and handle, and can be easily recycled. One of the most desirable features of CFS members, however, is that they may be shaped (cold-bent) to nearly any open cross section. This allows for the use of formal optimization strategies to find optimal shapes for the members' cross sections.

The goal of this work is to examine the role of boundary conditions on optimal CFS column cross sections, i.e. cross sections that maximize compressive capacity of a CFS column with a given length, coil width, and sheet thickness. In addition, we discuss the choice of longitudinal basis functions in the context of Finite Strip Method (FSM), the computational strategy used to explore different instability modes of a given cross section. As far as the optimization algorithm is concerned, the available options are: algorithms based on formal mathematical programming and those that are based-on principles of stochastic search. Gradient descent based solutions are highly sensitive to the initial design, but lead to more practical cross sections (e.g. symmetrical). The stochastic search algorithms, on the other hand, are computationally expensive but do a better job in exploring the design space while being relatively insensitive to the initial design. In this paper we choose a somewhat hybrid approach. We first start exploring the design space via a stochastic search algorithm. To arrive at practical designs we put constraints on the geometrical properties of the optimal cross section. We finally refine the near-optimal folding of the cross section through a few steps of the gradient descent optimization.

Keywords: Cold formed steel, General boundary condition, Direct strength method, Finite strip method, Genetic algorithm

1 Introduction

Among thin-walled structures, those that are composed of cold-formed steel members have become widespread in the practice of structural engineering due mostly to the increasing demand for economical and efficient structural elements. Recent theoretical developments on methodologies for the design and analysis of such members have also lead to a more extensive usage of cold-formed steel in building industry.
A number of scholars have conducted research on optimization of cold-formed steel cross section selection and design. Lu [1] embedded FSM in a genetic algorithm routine to optimize CFS purlins subjected to geometrical and strength constraints. Liu et al [2] used DSM and FSM along with Bayesian classification trees to optimize the nominal strength of cold formed steel cross sections. Leng et al [3] explored three optimization algorithms including steepest descent, genetic algorithm and simulated annealing to find cross-sections with maximum compressive strength for simply supported cold-formed steel columns of different lengths.
The goal of this work is to examine the role of boundary conditions on optimal CFS column cross sections. This study is therefore an extension of the work in [3] in the sense that it covers a variety of boundary conditions for the column. In addition, we discuss the choice of longitudinal basis functions in the context of FSM. Our computational experience (see also [3]) shows that gradient descent based solutions are highly sensitive to the initial design, but are more practical (i.e. lead to symmetrical cross sections). The stochastic search algorithms, on the other hand, are computationally expensive but do a better job in exploring the design space. They are also relatively insensitive to the initial design. In this paper we therefore use a hybrid strategy. We first explore the design space via a stochastic search algorithm. We then refine the near-optimal folding of the cross section through a few steps of the gradient descent optimization.

2 Finite Strip Method (FSM) for general boundary conditions

2.1 Basics

FSM is a semi-analytical method, in which a (prismatic) thin-walled member is discretized into a number of

longitudinal narrow strips. The interpolating functions in the transverse direction are assumed to be polynomials while judiciously chosen trigonometric functions are used in the longitudinal direction. These longitudinal basis functions are such that they satisfy the boundary conditions. One advantage of such a strategy is that it circumvents the need for discretization in the longitudinal direction and increases the computational efficiency to a great extent. The computational efficiency resulting from the choice of predefined shape functions comes in handy in cases where repetitive analyses must be performed. The reader interested in more details on FSM is referred to the well-known text by Cheung and Tham [4], and numerous papers and technical reports prepared by thin-walled structures research group at Johns Hopkins University (see [5] for example).

In this paper we use the open source software CUFSM [6]. As for longitudinal shape functions, we use analytically driven column buckling mode shapes. Having their basis in the mechanics of buckling, we believe these basis functions are more relevant in the stability analysis of plate assemblies with different boundary conditions (see also [4]). A quick look at FSM reveals that to switch from one set of longitudinal shape functions to another all one has to do is to re-calculate I_1 to I_5 integrals defined below [7]:

$$I_1 = \int_0^a Y_p Y_q dy\,, \qquad I_2 = I_3 = \int_0^a Y_p'' Y_q dy\,, \qquad I_4 = \int_0^a Y_p'' Y_q'' dy\,, \qquad I_5 = \int_0^a Y_p' Y_q' dy \tag{1}$$

where Y_ps are the longitudinal shape functions. One advantage of using buckling mode shapes as longitudinal shape functions is that, depending on the boundary condition in place, some of the integrals I_1 to I_5 need not be calculated as they are identically zero due to orthogonality properties of these mode shapes. The computed results for C-C boundary conditions for example are listed in Table 1.

Table 1: Clamped-Clamped integrals

Conditions	I_1	$I_2 = I_3$	I_4	I_5
$p^{(s)} = q^{(s)}$	$3a/2$	$-2\pi^2.p^2/a$	$8\pi^4.p^4/a^3$	$2\pi^2.p^2/a$
$p^{(a-s)} = q^{(a-s)}$	$5a/6$	$-a.k_p{}^2/2$	$a.k_p{}^4/2$	$a.k_p{}^2/2$
$p^{(s)} \neq q^{(s)}$	a	0	0	0
$p^{(s)} \neq q^{(a-s)}$	0	0	0	0
$p^{(a-s)} \neq q^{(s)}$	0	0	0	0
$p^{(a-s)} \neq q^{(a-s)}$	$a/3$	0	0	0

Superscripts: s → Symmetric & a-s→ Asymmetric

2.2 Identification of different buckling loads

In this paper we use Direct Strength Method (DSM) to calculate the compressive strength of a given CFS column. An important step in the application of Direct Strength Method (DSM) is the identification of global (Euler), local and distortional buckling loads for the particular cross-section under consideration. This can be done with help of modal identification strategies such as constrained Finite Strip Method (cFSM) [7]. Such strategies are, however, computationally demanding.

A signature curve in the context of stability analysis of open thin-walled cross sections using FSM is a plot of critical stress (or load), calculated using only one term (first term) in the trigonometric series, versus length of the member. For general boundary conditions (other than simply supported) the signature curve losses its meaning. To identify the critical loads for a general boundary condition, Ref. [7] suggests that either FSM be used with modes that lie in the neighborhoods of critical modes in the signature curve for the same column with simply supported boundary conditions (FSM@SIG- L_{cr}) or one follows the more accurate FSM@cFSM-L_{cr} strategy. The latter however calls for a constrained finite strip analysis and may prove expensive especially in the context of an optimization problem. We therefore adopt a strategy which is slightly different from the former but is similar to that when it comes to the computational expense.

Figure 1 depicts the critical loads calculated using "one-term" FSM analyses each performed with a different term ($p = m$) kept in the trigonometric series that is appropriate for the boundary condition in place. The horizontal axis represents a/p (physical length divided by p) and can therefore be denoted by "half-wave length" as it is done in a signature curve. We call this curve a pCurve to differentiate it from the signature curve. We then use this pCurve for the identification of different modes of instability as follows:

1. If there is at least two distinct minima, the first one is assumed to correspond to local buckling and the one with the least amount of critical buckling load among the others is considered to pertain to distortional buckling.
2. If one local minimum exists, it is assumed to correspond to local buckling if the associated critical length is less than the reference length, and to distortional buckling otherwise. In the first case, the

distortional buckling point is chosen to be first local minimum in derivative of pCurve (see Figure 1). If the minima in the derivative cannot be found, then tracking the reference length is pursued.

3. If no minimum exists at all, then the global buckling load is calculated using the physical length and the other two buckling modes will be ignored in the DSM calculations.

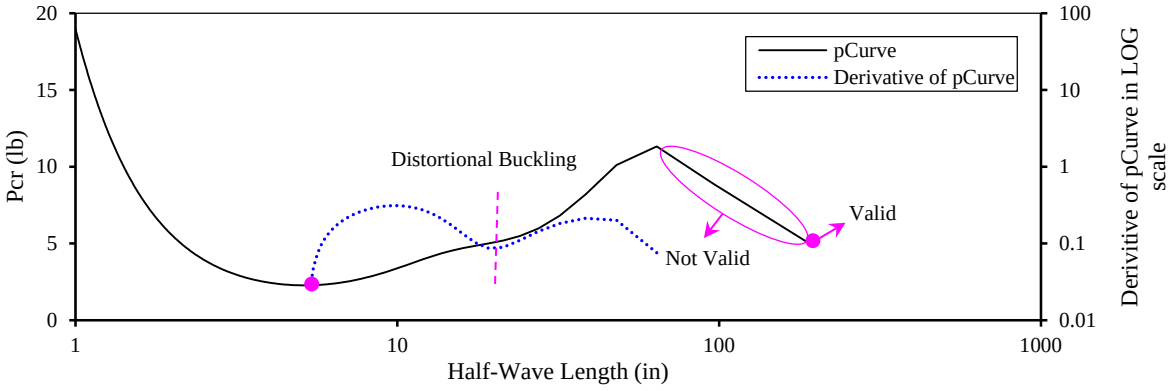

Figure 1: pCurve definition

3 Optimization method

3.1 Preliminary remarks

As was discussed in the introduction the search for cross sections with optimal compressive strength is done through a combination of a stochastic search algorithm, and the usual gradient descent optimization. Four different boundary conditions are considered in this paper, namely Clamped-Clamped, Clamped-Guided, Clamped-Free and Clamped-Simple (hereafter referred to as C-C, C-G, C-F and C-S respectively). The standard lipped channel section demonstrated in Figure 2 will be used as a first guess in the optimization process. The web height is 6.82in, and the upper and lower flanges each have a width of 1.57in. The lip length is 0.52in. This results in a coil width of 11.02in. The thickness is constant and equals 0.039in. The column is subjected to a uniform compressive stress. The Young's modules of steel sheets is assumed to be 30,458 ksi and the yield stress is 33 ksi.

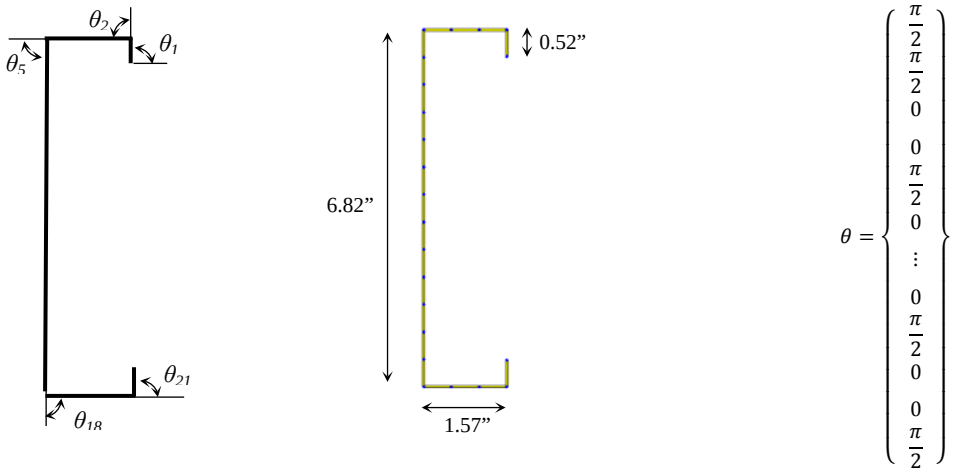

Figure 2: Lipped channel section

3.2 Problem formulation

We discretize the section into 21 equal width narrow strips. The turn angle θ_i is defined as the change in relative angle between the vector connecting point $i-1$ to point i and the local axis of the i^{th} element measured counter clockwise. We collect all these turn angles in a vector $\boldsymbol{\theta}$ as follows:

$$\boldsymbol{\theta} = [\theta_1, \theta_2, \cdots, \theta_{21}] \tag{2}$$

According to DSM [8] the nominal axial strength for flexural, torsional or flexural-torsional buckling P_{ne} can be calculated as follows:

$$P_{ne} = \begin{cases} \left(0.658^{\lambda_c{}^2}\right) P_y & if \quad \lambda_c \le 1.5 \\ \left(0.877/\,\lambda_c{}^2\right) P_y & if \quad \lambda_c > 1.5 \end{cases} \tag{3}$$

with $\lambda_c = \sqrt{P_y/P_{cre}}$ the non-dimensional column slenderness, $P_y = A_g F_y$ the squash load and P_{cre} the critical load associated with Euler (global) buckling. The nominal axial strength for local buckling is calculated as:

$$P_{nl} = \begin{cases} P_{ne} & if \quad \lambda_l \le 0.776 \\ \left[1 - 0.15\left(\frac{P_{crl}}{P_{ne}}\right)^{0.4}\right]\left(\frac{P_{crl}}{P_{ne}}\right)^{0.4} P_{ne} & if \quad \lambda_l > 0.776 \end{cases} \tag{4}$$

with $\lambda_l = \sqrt{P_{ne}/P_{crl}}$ and P_{crl} the critical load associated with local buckling. Finally, the nominal axial strength for distortional buckling is calculated from the following equation:

$$P_{nd} = \begin{cases} P_y & if \quad \lambda_d \le 0.561 \\ \left[1 - 0.25\left(\frac{P_{crd}}{P_y}\right)^{0.6}\right]\left(\frac{P_{crd}}{P_y}\right)^{0.6} P_y & if \quad \lambda_d > 0.561 \end{cases} \tag{5}$$

where $\lambda_d = \sqrt{P_y/P_{crd}}$ and P_{crd} is the critical load for the distortional buckling. The nominal strength of column is then considered to be the minimum of these values:

$$P_n = \min(P_{ne}, P_{nd}, P_{nl}) \tag{6}$$

The optimization problem can thus be defined as follows:

$$\begin{aligned} &minimize\{-P_n(\boldsymbol{\theta})\} \\ &\quad Subjected\ to: \ \boldsymbol{\theta} < \theta_{max} = \pi \\ &\qquad\qquad \theta_{min} = -\pi < \boldsymbol{\theta} \\ &\qquad\qquad \boldsymbol{C}_{overlap} = \mathbf{0} \\ &\qquad OR \quad \theta_i - \theta_{n-i+2} = 0, \quad Symmetric \\ &\qquad\qquad \theta_i + \theta_{n-i+2} = 0, \quad Anti - Symmetric \quad i = 2,3,\dots,11 \ \&\ n = 21 \end{aligned} \tag{7}$$

The constraints on the geometrical properties are added to arrive at practical designs (e.g. symmetric and anti-symmetric)

3.3 Solution strategy

Once the necessary equations and tools are available to evaluate $P_n(\boldsymbol{\theta})$ for any given design iteration $\boldsymbol{\theta}$, the next step would be to choose an optimization engine that can solve the optimization problem (7). In this paper we adopt the following hybrid strategy: a) use Genetic Algorithm to explore the design space thoroughly and arrive at solutions that are nearly optimal b) use gradient descent to improve the near-optimal folding obtained by GA. In what follows we briefly describe the optimization engines used in this paper. Reader interested in more details is referred to references [9], [10], [11] and [12].

3.3.1 Genetic Algorithm

A member of the class of evolutionary algorithms (EA), Genetic Algorithm (GA) mimics the process of natural evolution by transforming the design through a set of evolution-like actions: creation, mutation, selection, and crossover. GA begins by creating the initial population of creatures (the first generation). Each creature (individual) in the population is a double precision vector of turn angles created randomly biased to satisfy all bounds and constraint. Individuals within each generation are ranked based on the value of the fitness function (compressive strength in this paper). They are then used to generate the next generation in the following way. A number of individuals are directly moved to the next generation. These are known as "Elite" children; A fraction of the remaining individuals go through the crossover process while others are mutated to reduce the possibility of getting stuck in local minima before reaching the global one. This process will be repeated until the convergence occurs, that is the average change in fitness value is less than a predefined tolerance.

3.3.2 Active Set Algorithm

The optimal design obtained via GA is fed into an active set algorithm for a few final iterations aimed at fine tuning the design. The algorithm uses a sequential quadratic programming (SQP) method in which a quadratic programming (QP) subproblem is solved at each major iteration. To form the QP subproblem, the Hessian of the Lagrangian is approximated using a quasi-Newton updating strategy such as BFGS method.

4 Results

As was discussed above four boundary conditions, C-C, C-G, C-F and C-S are investigated. Also, to arrive at practical designs, the design space will be restricted to symmetric and anti-symmetric cross sections leading to cross sections that are more desirable from a manufacturing point of view.

4.1 Clamped-Clamped Column

The optimization framework discussed in Section 3.3 is used to optimize the cross section of a built-in (C-C) column of length 192in. Identification and separation of global, distortional and local buckling modes is done by following the strategies put forward in Section 2.2. The results are depicted in Figure 3. First, it is noted that the optimization procedure has increased the column capacity by a factor of 3.27. Second, it can be seen in Figure 3 (c) that for the given length and boundary condition, changing the manufacturability constraint from symmetric to anti-symmetric results in almost %10 present increase in the nominal strength. Finally, it is noted that, due to highly nonlinear relationship between the objective function and design parameters as well as the stochastic nature of the search, the hybrid optimization strategy may arrive at different solutions (Figure 3 (a) and (b)).

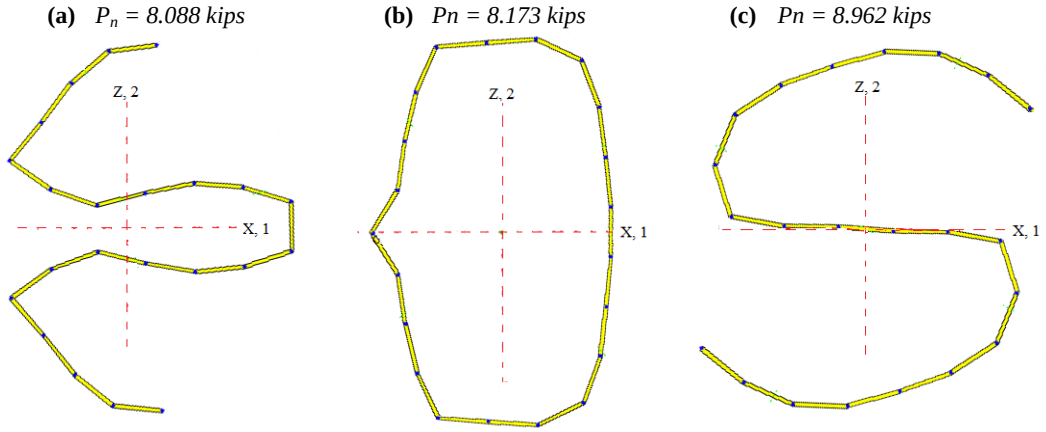

Figure 3: The optimized section for C-C condition, a & b) Symmetric, c) Anti-Symmetric

The cross sectional properties for the optimal shapes depicted in Figure 3 are listed in Table 2. The numbers suggest that, when compared with the lipped channel, the moments of inertia about principal axes are considerably closer in optimal cross sections. Results in Table 2 also indicate that the difference between the nominal compressive capacity obtained by adopting the pCurve strategy and that derived from a many-term finite strip analysis is negligible, confirming further that the pCurve strategy does a good job in identifying the critical buckling modes and their associated critical lengths.

Table 2: Cross sectional properties of lipped channel and optimized section in different Boundary condition

Section	BC	Fig.	I_{11} (in^4)	I_{22} (in^4)	C_w (in^6)	P_n (kips) *Approximate*	P_n (kips) *Many-term*
Lipped Chanel	C-C	2	2.8583	0.1411	1.3181	N/A	2.745 **L**
Hat Section		9a	0.4172	0.3360	0.5193	8.371 **E**	8.088 **E**
Circular		9b	0.8331	0.3538	4.3223	8.425 **E**	8.173 **E**
S- Section		9c	0.5903	0.3962	2.0939	9.187 **E**	8.962 **E**
Lipped Chanel	S-C	2	2.8583	0.1411	1.3181	N/A	1.794 **L**
Circular		10a	0.9550	0.3551	3.6487	5.252 **E**	5.006 **E**
Z- Section		10b	0.4667	0.4353	1.2196	6.450 **E**	6.105 **E**
Lipped Chanel	C-G	2	2.8583	0.1411	1.3181	N/A	1.009 **E**
Circular		10c	0.9005	0.3591	4.4609	2.706 **E**	2.545 **E**
Z- Section		10d	0.4593	0.4449	1.2773	3.389 **E**	3.143 **E**
Lipped Chanel	C-G	2	2.8583	0.1411	1.3181	N/A	0.242 **E**
Circular		10e	1.1950	0.3969	3.5767	0.767 **E**	0.702 **E**
Z- Section		10f	0.4478	0.4379	1.3395	0.807 **E**	0.765 **E**

N/A: Not applicable
E: Euler buckling is governing
D: Distortional buckling is governing
L: Local buckling is governing

4.2 Other Boundary Conditions

The same procedure is applied to the other types of boundary condition and the results are presented in Figure 4. It is seen that while symmetric optimal sections tend to have rounder corners, anti-symmetric optimal sections look more or less like Z or S sections. It is also noted that the optimization has increased the capacity of the

lipped channel by a factor of 3.4 for S-C boundary condition, a factor of 3.11 for C-G boundary condition and a factor of 3.16 for C-F boundary condition.

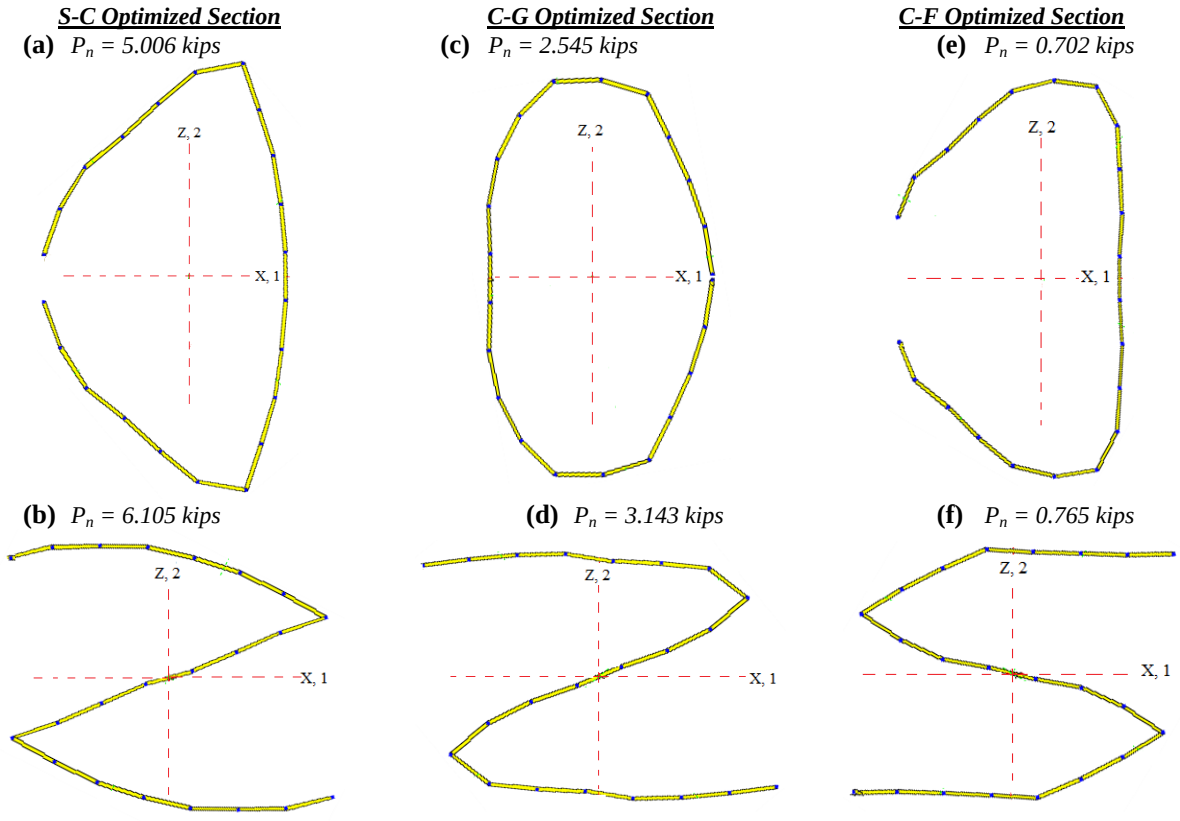

Figure 4: The optimized section with different BC

The numbers in Table 2 also indicate that the optimization engine is trying to increase the nominal compressive capacity by bringing closer together the moments of inertia about principal axes. This, whenever geometrical constraints allow (e.g. anti-symmetric cross sections) will result in nearly equal moments of inertia.

Table 3: Nominal and Critical buckling load (kips) of column in different BC

Section	BC	Fig.	P_{cre}	P_{crl}	P_{crd}	P_{ne}	P_{nl}	P_{nd}	P_n
Lipped Chanel	C-C	2	4.423	2.253	4.619	3.879	2.745	6.312	2.745 **L**
Hat Section		9a	10.569	42.627	19.852	8.088	8.088	12.045	8.088 **E**
Circular		9b	10.769	49.369	9.562	8.173	8.173	8.986	8.173 **E**
S- Section		9c	12.931	18.950	10.010	8.962	8.962	9.173	8.962 **E**
Lipped Chanel	S-C	2	2.333	2.252	4.587	2.046	1.794	6.290	1.794 **L**
Circular		10a	5.708	22.467	7.851	5.006	5.006	8.203	5.006 **E**
Z- Section		10b	7.043	11.336	5.291	6.105	6.105	6.763	6.105 **E**
Lipped Chanel	C-G	2	1.151	2.252	4.512	1.009	1.009	6.237	1.009 **E**
Circular		10c	2.901	10.184	1.733	2.545	2.545	3.733	2.545 **E**
Z- Section		10d	3.584	N	3.452	3.143	3.143	5.424	3.143 **E**
Lipped Chanel	C-F	2	0.276	2.253	4.120	0.242	0.242	5.951	0.242 **E**
Circular		10e	0.800	16.568	3.869	0.702	0.702	5.759	0.702 **E**
Z- Section		10f	0.872	5.368	2.311	0.765	0.765	4.373	0.765 **E**

N: Nonexistence
E: Euler buckling is governing
D: Distortional buckling is governing
L: Local buckling is governing

5 Conclusion

Optimal folding of open cold formed steel cross sections under compression were found by defining the design space in terms of a set of turn angels at a set of given points on the cross section of a standard lipped channel

with constant coil width. A hybrid strategy composed of a stochastic search algorithm, and a gradient descent engine was used to arrive at optimal designs. The nominal compressive strength of a given cross section was evaluated using a combination of Finite Strip Method (FSM) and Direct Strength Method (DSM). Two geometrical constraints, symmetry and anti-symmetry were imposed to arrive at designs that are more practical. The optimal folding was shown to be greatly influenced by the choice of boundary condition. Efficient modal identification strategies were used to circumvent the need for using detailed many-term or constrained finite strip analysis. While much work remains in terms of generalizing the methodologies proposed, the presented method was shown to perform satisfactory for the purpose of optimizing the cross sectional geometry of CFS members under compression.

6 References

[1] W. Lu, *Optimum Design of Cold-Formed Steel Purlines*, Publication TKK-TER-25, Helsinki University of Technology, Laboratory of Steel Structures, 2003.

[2] H. Liu, T. Igusa and B. W. Schafer, Knowledge-based global optimization of cold-formed steel columns, *Thin-Walled Structures,* 42(6), 785–801, 2004.

[3] J. Leng, J. K. Guest and B. W. Schafer, Shape optimization of cold-formed steel columns, *Thin-Walled Structures,* 49(12), 1492–1503, 2011.

[4] Y. K. Cheung and L. G. Tham, *The Finite Strip Method*, CRC Press, 1997.

[5] Z. Li, *Buckling Analysis via Finite Strip Method and theoretical Extension of the Constraint Finite Strip Method For General Boundary Condition*, Johns Hopkins University, Baltimore, 2009.

[6] S. Adany and B. W. Schafer, A full modal decomposition of thin-walled, single-branched open cross-section members via the constrained finite strip method, *Journal of Constructional Steel Research,* 8(1), 12-29, 2008.

[7] Z. Li and B. W. Schafer, Buckling analysis of cold-formed steel members with general boundary conditions using CUFSM: conventional and constrained finite strip methods, in *Proceedings of the 20th International Specialty Conference on Cold-Formed Steel Structures*, Saint Louis, 2010.

[8] North American Specification, Appendix 1. *Design of Cold-Formed Steel Structural Members Using the Direct Strength Method*, Washington, American Iron and Steel Institute, 2007.

[9] D. E. Goldberg, *Genetic Algorithms in Search, Optimization, and Machine Learning*, Boston, Addison-Wesley Longman Publishing Co., 1989.

[10] P. W. M. a. M. W. Gill, *Practical Optimization*, London, Academic Press, 1981.

[11] R. Fletcher and M. J. D. Powell, A Rapidly Convergent Descent Method for Minimization, *Computer Journal*, 6(2), 163-168, 1963.

[12] M. J. D. Powell, Variable Metric Methods for Constrained Optimization, in *Mathematical Programming: The State of the Art, A. Bachem, M. Grotschel and B. Korte, eds.*, 288-311, Springer-Verlag, Berlin,1983.